scientific **data**

DATA DESCRIPTOR

Check for updates

Circadian rhythmicity and reinforcement processing: a dataset of MRI, fMRI, and behavioral measurements

Patrycja Scislewska [1] ✉, Michal Rafal Zareba[2], Julia Lengier[1], Aaron E. Schirmer[3], Piotr Bebas[1] & Iwona Szatkowska[4]

Circadian rhythmicity is a complex phenomenon that influences human behavior, emotionality and brain activity. A detailed description of individual differences in circadian rhythmicity could inform the design of educational systems, shift-worker schedules, and daily routines. Here we present a comprehensive dataset for studying diurnal rhythms and their relationship with human behavior. Thirty seven male participants (aged 20–30) filled in validated psychometric questionnaires assessing characteristics of the circadian rhythm, sleep quality, emotionality, personality traits, reward-punishment processing and attention deficits. Moreover, we acquired high-resolution anatomical T1-weighted images using magnetic resonance imaging (MRI), B0 fieldmaps for distortion corrections, and functional MRI (fMRI) during the Monetary Incentive Delay (MID) task, which is a common paradigm to assess human neural reinforcement processing. All files are organized in Brain Imaging Data Structure (BIDS) and openly available on OpenNeuro.org. Validation confirmed the high quality of the described dataset. The various psychological measures combined with neuroimaging data provide a strong foundation for exploring emotionality, affective processing, and attention in the context of brain activity and circadian influences.

Background & Summary

Circadian rhythmicity in humans is a complex phenotype that encompasses multiple dimensions. Full description of the daily rhythm requires a characterization of three distinct components: chronotype, distinctness (fluctuations of the perceived energy level during the day, i.e., amplitude of diurnal variations in mood, motivation, and cognitive functioning), and morning affect (energy and alertness soon after waking, irrespective of wake-up time)[1]. However, the majority of investigations used a unidimensional assessment of morningness-eveningness (chronotypes)[2,3]. In these studies, eveningness has been associated with negative emotionality, propensity to depression and anxiety, neuroticism, and reduced reward responsiveness[4–8]. Additionally, altered reward-related brain functioning has been observed in people with evening chronotype[9–12]. Neuroticism, as well as propensity to depression and anxiety, are associated with motivation-related deficits, which are reflected in decreased responsiveness to rewarding stimuli, reduced approach-related behaviors, enhanced sensitivity to punishment, and increased avoidance behavior[13]. In addition, previous research revealed that, despite the people with evening chronotype showing higher intelligence[14–16] and cognitive ability[17], they have worse academic achievements[18,19]. These findings suggest that incentive motivation is modulated by the morningness-eveningness dimension of the circadian system. Recent research has also suggested the importance of distinctness and morning affect for these processes[20,21]. For example, distinctness negatively correlates with life satisfaction and positively correlates with negative emotionality[8,20,22–24]. Moreover, our recent study revealed that gray matter volume and cortical thickness in the left primary visual cortex are negatively correlated with the distinctness, regardless of chronotype.

[1]University of Warsaw, Faculty of Biology, Warsaw, Poland. [2]Department of Basic and Clinical Psychology and Psychobiology, Jaume I University, 12-006, Castellon de la Plana, Spain. [3]Department of Biology, Northeastern Illinois University, 5500 N. St. Louis Ave, Chicago, IL, 60625, USA. [4]Laboratory of Emotions Neurobiology, Nencki Institute of Experimental Biology, Polish Academy of Sciences, 02-093, Warsaw, Poland. ✉e-mail: p.scislewska@uw.edu.pl

Furthermore, the association of distinctness with gray matter volume in the right middle temporal gyrus differs between morning- and evening-chronotype groups[25]. As both areas have been implicated in the processing of positive and negative emotional stimuli, the existing evidence points toward the important role of circadian dimensions other than chronotype in reinforcement processing. Nevertheless, such studies remain sparse.

To further explore these aspects of human diurnal rhythmicity, we conducted a study with two main components: examining the subjects' behavior using psychometric questionnaires and measuring brain activity using functional Magnetic Resonance Imaging (fMRI). The characteristics of the individual circadian rhythmicity were assessed using the Morningness-Eveningness Stability-Scale improved (MESSi) questionnaire, and sleep quality was controlled using the Athens Insomnia Scale. We recruited 37 male participants (aged 20–30) and collected diverse psychometric data. This allowed us to assess individual differences in sensitivity to punishment and reward, personality traits, positive and negative affect, behavioral inhibition system and behavioral activation system (BIS/BAS), anxiety levels, and attention deficits (for details, see: Methods). Additionally, participants also completed an fMRI version of Monetary Incentive Delay task (MID task), which is a widely used paradigm for assessing reward- and punishment-motivated behavior[26,27].

Although we shared the preliminary results of our analyses as a preprint titled "High distinctness of circadian rhythm is related to negative emotionality and enhanced neural processing of punishment-related information in men"[28], the dataset offers significant opportunities for reuse and extension. The broad range of collected psychological data provides a foundation for research focusing on various aspects of human emotionality, affective processing, or even attention disorders.

All of the described data are openly available on OpenNeuro.org, organized according to the standardized Brain Imaging Data Structure (BIDS) format, which facilitates integration with other datasets and opens novel directions for future research projects.

Methods

Participants. We invited 37 healthy young men (age 20–30) to participate in the study of circadian-related differences in affective processing and psychological traits. Participants were reached via social media advertisements and local flyers. Subjects were screened before data collection to ensure that all had normal or corrected-to-normal vision, were drug-free, and had no self-reported history of neurological or psychiatric disorders, as well as MRI contraindications. Recruited participants were compensated for their time with a guaranteed payment of 50 PLN (Polish Zloty, 1 PLN equals 0.30 USD). To enhance participants' motivation to engage in the task, we informed them that the total final payout would depend on their performance in the experiment (up to 110 PLN; 30 USD), and would be received after the experimental session.

The described protocol was approved by the Rector's Committee for the Ethics of Research Involving Human Participants at the University of Warsaw (decision no. 230/2023) and was performed in accordance with the Declaration of Helsinki. Written informed consent prior to experimentation was obtained from all participants.

Procedures. *Overview.* The described study consisted of two parts: an online psychometric assessment and an in-person MRI/fMRI scanning session. At the beginning of the study, all participants received individual, 4-digit, random ID codes, which allowed us to combine both psychological and neurobiological data while maintaining participants' anonymity. All used questionnaires were distributed to the participants using the Psytoolkit online tool[29,30] (for details, see: Procedures, Behavioral data collection). Participants were asked to complete all surveys before the scanning session. During the appointment, participants underwent a mock MRI training session while performing the MID task (for details, see: Procedures, Monetary Incentive Delay task). This first pre-scanning attempt allowed them to become familiar with the task, to learn the values assigned to specific graphical symbols (cues), and to practice using the response pads (each subject was to respond using the index finger of the right hand). Moreover, during this mock session, we measured the participants' reaction times to set their individual threshold, ensuring 60% efficiency in the MID task.

Following the training, an actual scanning session was conducted. The entire scanning session lasted approx. 20 minutes. Each session consisted of an anatomical T1-weighted scan (6 min), a fieldmap, and a functional scan during the MID task (13 min comprising 60 trials of 13 seconds each) (for details, see: Procedures, Neuroimaging data collection).

All described procedures were conducted during two weeks in summer, all MRI examinations were carried out from 1 PM to 5 PM.

Behavioral data collection. During the study, we collected data on (I) subjective characteristics of the circadian rhythms, using the Polish version of the Morningness-Eveningness-Stability-Scale improved (MESSi) questionnaire[20,31], (II) insomnia symptoms, using the Athens Insomnia Scale (AIS) questionnaire[32], (III) individual differences in reinforcement processing, using the Sensitivity to Punishment and Sensitivity to Reward Questionnaire (SPSRQ[33,34]), (IV) personality traits, using NEO-Five Factor Inventory (NEO-FFI[35,36]), (V) behavioral inhibition and activation tendencies, using Behavioral Inhibition System and Behavioral Activation System (BIS/BAS[37,38]), (VI) positive and negative affect, using Positive and Negative Affect Schedule (PANAS[39,40]), (VII) generalized anxiety symptoms, using Generalized Anxiety Disorder (GAD-7[41]) and (VIII) attention deficit and hyperactivity symptoms, using Adult ADHD Self-Report Scale (ASRS[42,43]).

Monetary incentive delay task. Monetary Incentive Delay task (MID task) is a common method of assessing motivated behavior[26,27].

During the task performance, participants have to rely on previously learned associations between the cues and monetary outcomes. Therefore, the task is assumed to activate brain regions involved in reward-punishment
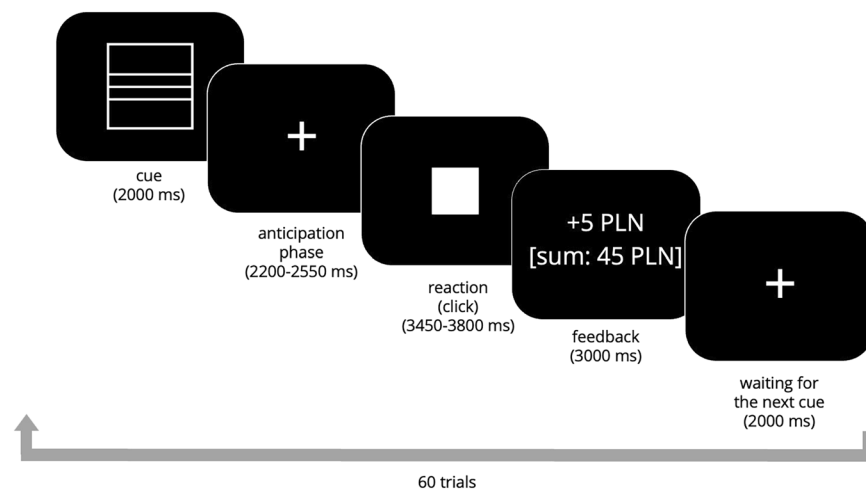
Fig. 1 A schematic of Monetary Incentive Delay (MID) task used in the described study.

processing, as well as attention and working memory, such as prefrontal cortex (PFC). The experiment was performed using Presentation software (Version 23.0, Neurobehavioral Systems, Inc., Berkeley, CA, www.neurobs.com).

Each trial in the MID task consists of 5 stages, as shown in Fig. 1. At the beginning of each trial, a graphic symbol - cue - with an assigned monetary value is displayed. After the cue, a fixation cross is shown. In the next stage, a screen with a white, filled square appears - this signals that the subject should click the button on the response pad as quickly as possible to get a reward/avoid a punishment (depending on the previously displayed cue). After the reaction (click), the participant gets a feedback screen, displaying the result of a given trial and the total money amount collected so far. After the feedback, another fixation cross appears, and the next trial begins. One trial lasts 13 seconds, and this is repeated for 60 cycles. The anticipatory screen and the reaction screen were defined with 8 pseudo-random combinations of their durations to avoid participants learning the clicking rhythm. The duration of each trial is kept the same by having these combinations always add up to 6 seconds (e.g. 2200 ms + 3800 ms or 2550 ms + 3450 ms), (Fig. 1).

To study the aspects of neural reinforcement processing (reward and punishment), we designed an experiment consisting of the MID task (for rewards and punishment processing) combined with the oddball paradigm (for keeping participants focused on cue processing). The task consisted of 60 trials: 28 reward trials (square with 3 lines represents big win: +5 PLN, square with 1 line represents a small win: +1 PLN), 28 punishment trials (circle with 3 lines represents big loss: –5 PLN, circle with 1 line represents small loss: –1 PLN), and 4 oddball trials to maintain participants' focus (triangle, +/−10 PLN), where the expected behavior was to inhibit the clicking reaction. The sequence in which the cues were presented in the task was pseudo-randomized but consistent across all subjects. A summary of cues is shown in Fig. 2.

Neuroimaging data collection. The MRI data was acquired using a 3.0 Tesla MAGNETOM Prisma Siemens scanner at the Laboratory of Brain Imaging (LOBI), Neurobiology Center at the Nencki Institute of Experimental Biology Polish Academy of Science. Scans were performed using a 32-channel head coil. For each subject, we obtained a high-resolution T1-weighted anatomical scan using Gradient Echo with Inversion Recovery sequence (GR\IR). Scans parameters were: slice thickness = 1 mm, echo time (TE) = 0.00296 s, repetition time (TR) = 2.3 s, inversion time (TI) = 0.9 s, isotropic voxel size = $1 \times 1 \times 1$ mm3, matrix 208×240 with 256 slices. During the performance of the MID task, functional T2*-weighted scans sensitive to blood-oxygenation-level-dependent (BOLD) contrast were collected. The fMRI data were acquired using an echo-planar imaging (EPI) sequence with a Siemens' proprietary multiband implementation (syngo MR XA30), with a multiband acceleration factor of 2. The scan parameters were as follows: TR = 2.0 s, TE = 0.03 s, flip angle = 70°, phase encoding direction AP (j-), isotropic voxel size = $2.5 \times 2.5 \times 2.5$ mm³, matrix = 84×84, with 60 slices per volume and 397 volumes in total (duration of fMRI scan = 13.23 min). Moreover, to correct for susceptibility-induced distortions in the fMRI data, we collected a single volume spin-echo EPI B0 fieldmaps. These scans were acquired in anterior-to-posterior (AP) and posterior-to-anterior (PA) phase encoding directions. The scan parameters for both directions were: TE = 0.066 s, TR = 8.0 s, flip angle = 90°, slice thickness = 2.5 mm, spacing between slices = 2.5 mm, isotropic voxel size = $2.5 \times 2.5 \times 2.5$ mm³, matrix = 84×82, with 60 slices per volume. Original DICOMs were converted to the NIfTI format using the dcm2niix software package[44]. To maintain participants' anonymity, scans were defaced using pydeface[45].

In the task design, the onset of the first trial was intentionally delayed by 10 seconds to allow for synchronization with fMRI acquisition and the collection of dummy volumes typically excluded due to signal instability. Specifically, the task script was configured to wait for the first scanner trigger (TTL pulse) before presenting a fixation screen, which served as a temporal anchor to align stimulus presentation with stabilized BOLD signal acquisition. In our dataset, we provided event files in two versions - a ready to use clean version of onset time, duration, and trial type for analysis of the anticipatory phase, and a complete set of trial logs, including all
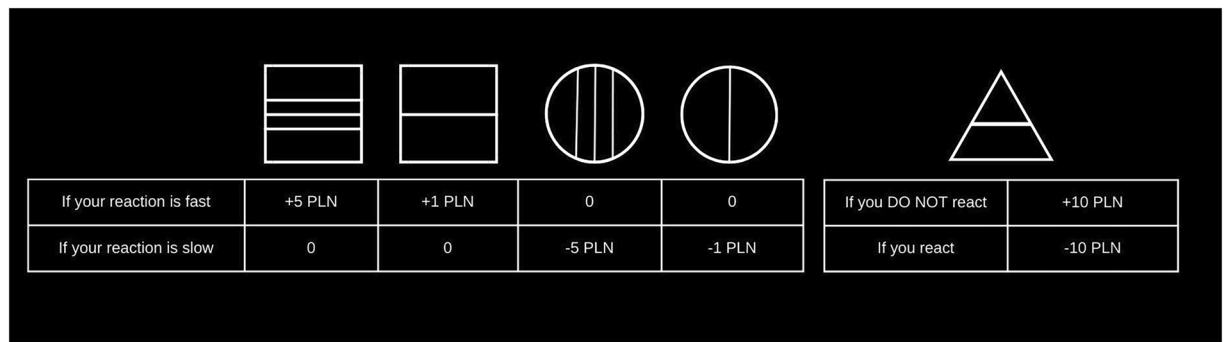
Fig. 2 Graphical cues from the Monetary Incentive Delay (MID) task. Participants learned the monetary values of these cues during a training session. At the beginning of the scanning session, participants were shown this screen to refresh the meaning of each cue. However, during the MID task, participants had to rely on their memory.

60 trials per participant and detailed information for each trial, including onset, duration, reaction time, and trial outcome (e.g., gain/loss). These datasets will allow future users to conduct extended analyses if desired.

Data Records

All described data records are publicly available as OpenNeuro Dataset ds005479 (https://openneuro.org/datasets/ds005479/versions/1.1.0)[46]. The dataset includes a README file, a dataset description, a participant file with psychometric data, and neuroimaging data. Neuroimaging files are organized according to the Brain Imaging Data Structure (BIDS)[47], within folders for each participant (<sub-XX>) and specific subfolders scheme: (1) <anat> (raw, defaced anatomical T1-weighted MRI scans), (2) <func> (raw BOLD data and an event file (.tsv file) listing onset times, durations, and types of stimuli), and (3) <fmap> (raw B0 fieldmaps acquired in two phase encoding directions (AP and PA)). Additionally, each subfolder includes a.json file with technical details about the corresponding NIfTI files.

Technical Validation

To ensure the technical validation of our behavioral and neuroimaging data, we conducted a series of comprehensive analyses. For details about the psychometric dataset, see: Technical Validation, Behavioral data. Neuroimaging data quality was evaluated using a set of image quality metrics: Contrast-to-noise ratio (CNR), framewise displacement (FD), DVARS, temporal Signal-to-noise ratio (tSNR) (for details, see: Technical Validation, Neuroimaging data). Here, we present the results of these validation procedures across all 37 participants. We note that no data were excluded from the published dataset. Users are encouraged to make their own decisions regarding the exclusion or use of specific subgroups of participants, and the provided metrics may be helpful in making those decisions.

Behavioral data. The described dataset contains psychometric properties collected from 37 men (aged 20–30). There are no missing values or duplications. In Table 1. we provided descriptive statistics for the dataset, including the mean, standard deviation (SD), minimum and maximum scores obtained by participants, first quartile (Q1, 25%), second (Q2, 50%), and third quartile (Q3, 75%), skewness, kurtosis, and results of the Kolmogorov-Smirnov (KS) test for normality (D-statistics and p-values). According to the KS test, all variables are normally distributed (p-value > 0.05). In Fig. 3. histograms and corresponding density curves are shown for all variables. For all examined psychometric scales, higher scores indicate greater intensity of the corresponding trait.

Neuroimaging data. The dataset includes raw MRI data, however, to validate the quality of MRI data, we calculated all necessary metrics using preprocessed images. All procedures were performed using FSL tools and custom scripts, as described below. Users are encouraged to apply their own preprocessing steps to tailor the images to their specific analytical approaches.

Fieldmap processing. Spin Echo Field Maps were collected with reversed phase-encoding blips, resulting in pairs of images with distortions going in opposite directions: anterior-to-posterior (AP) and posterior-to-anterior (PA) phase encoding. From these pairs, the susceptibility-induced off-resonance field was estimated using FSL[48], the two images were combined into a single corrected one (fslmerge and topup tools).

Anatomical data processing. T1-weighted anatomical scans were preprocessed using the fsl_anat pipeline in FSL. Original images were reoriented to match the standard MNI152 orientation using fslreorient2std. Non-brain regions were automatically cropped from the image using robustfov. The brain was extracted using a BET tool. Intensity inhomogeneities caused by RF/B1 field non-uniformity were corrected using the tissue segmentation step in FAST, which also segmented the image into gray matter (GM), white matter (WM), and cerebrospinal fluid (CSF) compartments. Anatomical images were registered to the MNI152 standard space using linear registration (FLIRT) with 12 degrees of freedom and spline interpolation. This affine transformation was

	Mean	SD	min	25%	50%	75%	max	Possible range (min-max)	Skewness	Kurtosis	KS statistics (D-statistics)	KS p-value
Age	24.432	2.089	20.0	23.0	25.0	25.0	30.0	—	0.208	0.530	0.165	0.236
Distinctness	18.243	3.068	10.0	17.0	18.0	20.0	25.0	5–25	−0.625	0.711	0.144	0.389
Eveningness	18.622	4.651	10.0	15.0	20.0	22.0	24.0	5–25	−0.745	−0.902	0.184	0.143
Morning affect	14.27	4.953	5.0	10.0	14.0	19.0	24.0	5–25	0.203	−0.942	0.116	0.656
Sensitivity to punishment	4.73	3.339	0.0	2.0	5.0	7.0	11.0	0–14	0.271	−0.937	0.118	0.643
Sensitivity to reward	4.595	1.691	2.0	3.0	4.0	6.0	8.0	0–10	0.097	−0.955	0.151	0.334
Neuroticism	25.216	7.983	13.0	19.0	25.0	32.0	41.0	0–48	0.278	−1.070	0.143	0.398
Extraversion	27.027	7.481	12.0	22.0	26.0	32.0	42.0	0–48	0.099	−0.569	0.072	0.984
Openness	31.351	6.672	15.0	26.0	33.0	36.0	42.0	0–48	−0.502	−0.522	0.138	0.441
Agreeableness	29.351	7.166	12.0	26.0	30.0	34.0	41.0	0–48	−0.801	0.066	0.131	0.511
Conscientiousness	27.973	7.489	14.0	23.0	28.0	31.0	46.0	0–48	0.248	−0.167	0.123	0.587
GAD	5.622	3.294	0.0	3.0	6.0	7.0	13.0	0–21	0.264	−0.378	0.149	0.352
Positive affect	33.027	6.768	16.0	30.0	33.0	36.0	50.0	10–50	−0.203	0.880	0.148	0.359
Negative affect	19.757	5.58	11.0	16.0	18.0	25.0	30.0	10–50	0.321	−0.947	0.164	0.244
BAS drive	9.351	2.7	5.0	7.0	9.0	11.0	16.0	4–16	0.47	−0.302	0.119	0.625
BAS fun seeking	10.595	1.691	7.0	9.0	11.0	12.0	14.0	4–16	−0.323	−0.524	0.175	0.182
BAS reward	14.541	2.567	9.0	13.0	15.0	16.0	19.0	5–20	−0.387	−0.375	0.121	0.612
BIS	19.459	4.161	8.0	17.0	19.0	23.0	27.0	7–28	−0.42	0.15	0.108	0.744
AIS	5.595	3.166	1.0	3.0	5.0	7.0	16.0	0–24	1.092	1.578	0.125	0.565
ASRS	34.378	10.505	18.0	26.0	32.0	41.0	61.0	0–72	0.473	−0.423	0.112	0.703

Table 1. The descriptive statistics for all psychometric variables from the dataset. Psychometric parameters were assessed using the Morningness-Eveningness-Stability-Scale improved questionnaire (MESSi[20,31]) with subscales of Distinctness, Eveningness, and Morning affect, the Sensitivity to Punishment and Sensitivity to Reward Questionnaire (SPSRQ[33,34]), NEO-Five Factor Inventory (NEO-FFI[35,36]) with subscales of Neuroticism, Extraversion, Openness, Agreeableness, and Conscientiousness, Generalized Anxiety Disorder (GAD-7[41]), Positive and Negative Affect Schedule (PANAS[39,40]) Behavioral Inhibition System and Behavioral Activation System (BIS/BAS[37,38]) with subscales of BAS drive, BAS fun seeking, and BAS reward responsiveness, the Athens Insomnia Scale questionnaire (AIS[32]), and Adult ADHD Self-Report Scale (ASRS[42,43]). Abbreviations: SD - standard deviation, min - minimum score, max - maximum score, KS - Kolmogorov-Smirnov test.

then used as the initialization for nonlinear registration with FNIRT, using the standard T1_2_MNI152_2mm.cnf configuration.

The quality of images was evaluated by calculating the Contrast-to-Noise ratio (CNR). All participants exhibited high CNR scores (Fig. 4a) - the contrast between gray and white matter is approximately 4.4 times greater than the background noise, confirming that the quality of described images is sufficient to reliably distinguish between GM and WM.

Functional data processing. Preprocessing of the functional images included motion correction (MCFLIRT tool), B0 inhomogeneity correction, intensity normalization, high-pass temporal filtering (90 s cutoff), registration to structural image (boundary-based registration; BBR) and registration to the MNI152 standard space, all performed in this order in FEAT FSL. To preserve image details, no spatial smoothing (FWHM) was applied. Our functional scans had a TR of 2 seconds and used a multiband factor of 2, which minimized slice timing offsets, thus the slice timing correction was not applied as well. However, we would like to emphasize that the described preprocessing pipeline is used only for assessing the data quality of the described dataset. We encourage all potential users to use their own preprocessing pipelines, tailored to their needs, selected data analysis method, and research goal.

The quality of functional images was assessed using three types of metrics: framewise displacement (FD) and DVARS to detect motion artifacts, temporal Signal-to-Noise ratio (tSNR) to evaluate the stability of the BOLD signal over time. We began examining the functional image quality using FD, which tracks head movement, and DVARS, which tracks changes in image intensity relative to the previous volume(s)[49,50]. Both metrics were calculated using fsl_motion_outliers tool, applying the default outlier threshold of the 75th percentile +1.5 times the interquartile range (IQR). For better interpretability, we scaled DVARS, by dividing the raw DVARS by mean signal intensity and multiplying by 100%.

There is no universally accepted threshold for movement, but FD thresholds between 0.2 and 0.5 mm are commonly used[50,51]. In the described dataset, both FD and DVARS values were low - FD was mostly < 0.05 mm, scaled DVARS < 0.3%, which indicates minimal head motion and high quality of data (Fig. 4b,c).

For calculating the temporal Signal-to-Noise ratio (tSNR), a metric for signal stability, we used both B0 field-corrected and uncorrected images. Individual and group-level tSNR maps were generated by dividing the mean of a time series by its standard deviation using fslmaths and aligned to the MNI152 standard template using FSL's FLIRT. Higher tSNR values reflect better stability of the BOLD signal over time. For visualization,
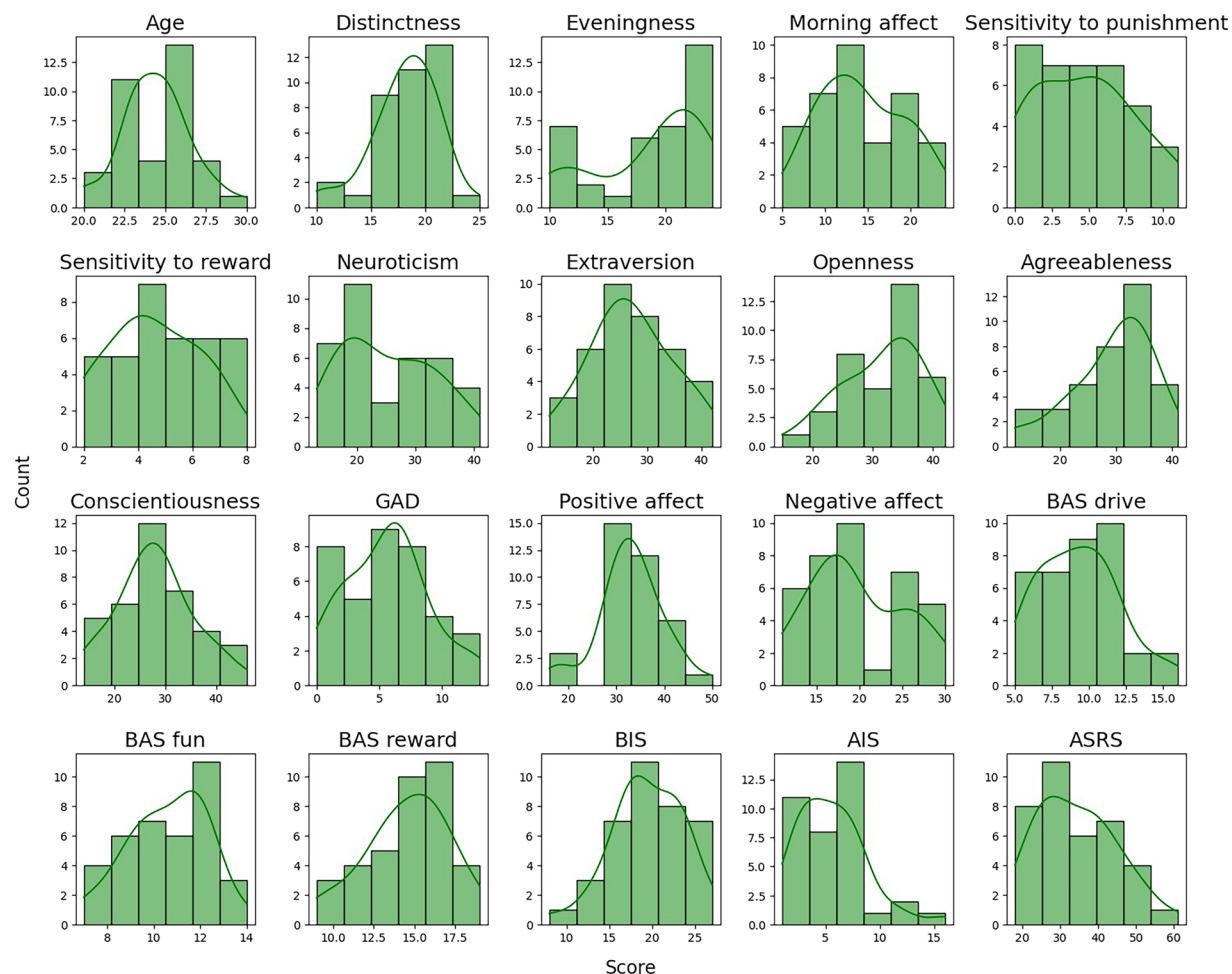
Fig. 3 Histograms and density curves for all variables in the described dataset. For ease of comparison, each scale was divided into 6 bins. Psychometric parameters were assessed using the Morningness-Eveningness-Stability-Scale improved questionnaire (MESSi[20,31]) with subscales of Distinctness, Eveningness, and Morning affect, the Sensitivity to Punishment and Sensitivity to Reward Questionnaire (SPSRQ[33,34]), NEO-Five Factor Inventory (NEO-FFI[35,36]) with subscales of Neuroticism, Extraversion, Openness, Agreeableness, and Conscientiousness, Generalized Anxiety Disorder (GAD-7[41]), Positive and Negative Affect Schedule (PANAS[39,40]) Behavioral Inhibition System and Behavioral Activation System (BIS/BAS[37,38]) with subscales of BAS drive, BAS fun seeking, and BAS reward responsiveness, the Athens Insomnia Scale questionnaire (AIS[32]), and Adult ADHD Self-Report Scale (ASRS[42,43]).

a threshold of tSNR > 30 was applied to the mean tSNR map to present regions with the highest signal stability (Fig. 5.). We observed that tSNR was high and relatively uniform across the whole brain.

It is worth mentioning here that functional images after or B0 inhomogeneities exhibited higher tSNR values compared to those without distortion correction (Fig. 4d), which underlines the importance of using fieldmaps (provided in the described dataset) to improve the quality of signals.

To confirm the task-related brain activation, we calculated the mean single-trial activation estimates using the Least Squares - Separate (LSS) approach implemented in SPM. We expected to observe the task-related responses in the visual cortex and motor cortex. For each trial, we specified the separate GLM where the trial of interest was modeled independently, all other trials - jointly, and six motion regressors were included as covariates. Individual beta maps were generated for each of the trials, and a mean beta map was computed by averaging across trials.

Consistent with this prediction, we found that the average response across single trials was associated with increased activation in the visual and motor cortices. This not only reflects the expected activational effects of the MID task but also confirms the accuracy of the provided trials' timing (Fig. 6).

Usage Notes

The described dataset consists of psychological data (on circadian rhythmicity, insomnia symptoms, personality traits, affective processing and emotion processing) and neuroimaging data obtained during performing Monetary Incentive Delay (MID) task from 37 young male participants. All data are organized in the BIDS structure. All required BIDS fields are included in the dataset, and the structure is fully compliant with the BIDS
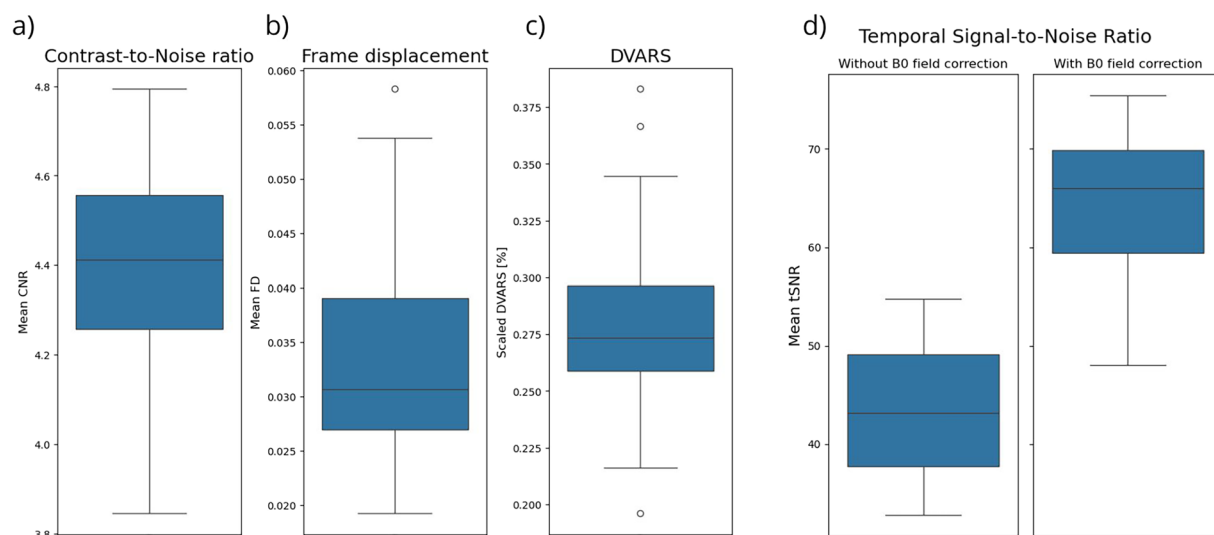
Fig. 4 MRI data quality metrics. (**a**) Anatomical data quality was assessed using Contrast-to-Noise ratio (CNR). Obtained CNR scores suggest that quality of T1-weighted images is sufficient for distinguishing tissues and suitable for structural analysis. (**b**) Mean framewise displacement (FD) - metric that detects motion artefacts in functional data. Low values (mostly < 0.05 mm) indicate minimal head movement. (**c**) Mean DVARS - metric that evaluates signal stability over time in functional data. Here we present the average percentage change in signal intensity between consecutive time points, normalized to the mean signal intensity. Low values indicate minimal signal fluctuations, which suggests high-quality, low-motion data. (**d**) Mean tSNR. Values for functional data with B0 field correction applied are notably higher in comparison with functional data without this correction. This underscores the importance of using the fieldmaps as a crucial step in preprocessing.
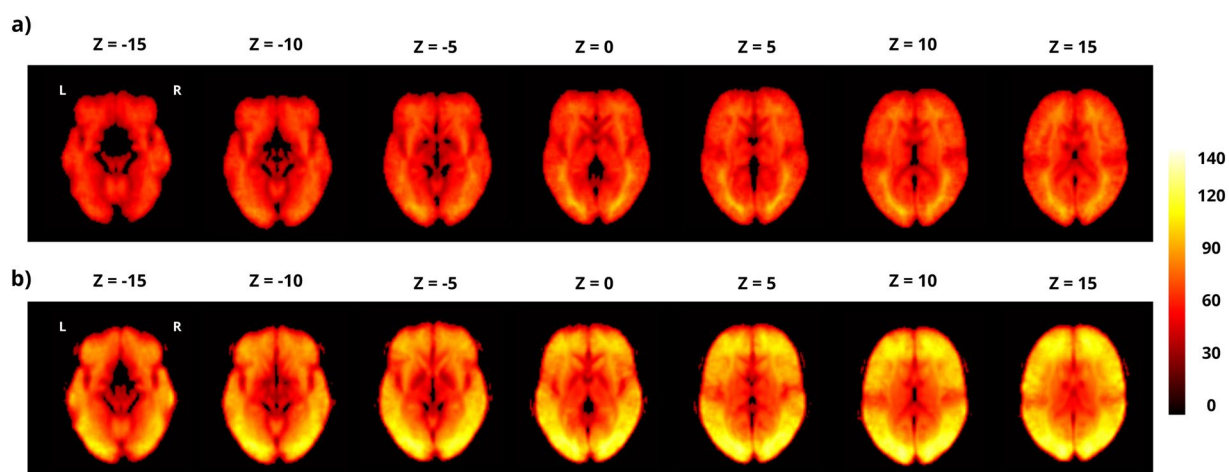
Fig. 5 Temporal Signal-to-Noise ratio (tSNR) averaged maps. High values of tSNR indicate a high-quality signal. The tSNR is relatively uniform across the whole brain. (**a**) Map prepared using functional data without distortion correction. (**b**) Map prepared using functional data with B0 inhomogeneity correction applied.

specification. The metadata warnings flagged by the OpenNeuro validator refer only to optional fields that were not recorded during acquisition (e.g., extended scanner information). While these fields are not mandatory, their absence does not affect the validity, completeness, or usability of the dataset.

Data were collected in order to investigate the intriguing relationship between individual circadian rhythms and affective processing. Preliminary results of our analyses are available as a preprint titled "High distinctness of circadian rhythm is related to negative emotionality and enhanced neural processing of punishment-related information in men"[28]. The paper is currently under peer review. However, the dataset includes a broad range of psychological traits, making it potentially useful for research in other focus areas. No data were excluded from the published dataset, so users can make their own determinations about exclusions.

However, it should be acknowledged that the dataset includes only male participants within a narrow age range, which limits the generalizability of the findings. Future studies should aim to include more diverse samples with respect to gender, age, cultural background, and circadian rhythm characteristics.
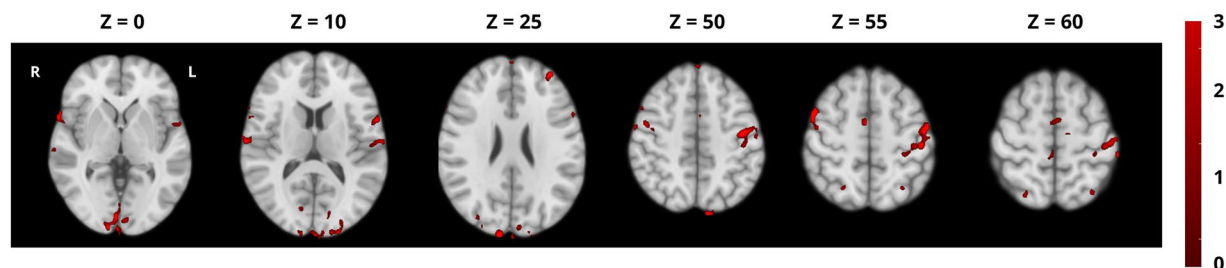
Fig. 6 Mean single-trial activation estimates. Single-trial beta estimates were obtained using a Least Squares - Separate (LSS) approach implemented in SPM. The presented activation map confirms the expected engagement of the motor and visual cortices during the MID task. The figure shows results from one representative participant on the MNI152 standard brain template. Results for all participants can be found in the Derivatives folder in the dataset. Coordinates were selected for optimal visualization.

Data are publicly available under a Creative Commons CC0 license at OpenNeuro: https://openneuro.org/datasets/ds005479/versions/1.1.0.

Code availability

To ensure reproducibility and transparency, the code used to perform the technical validation is available on Github: https://github.com/PatrycjaScislewska/Circadian_MRI_dataset. The repository contains custom Python notebooks and Bash scripts to run the open-source FSL tools (fsl_motion_outliers, fslmaths, fslmeans, fslstats).

References

1. Randler, C. Ontogeny of morningness–eveningness across the adult human lifespan. *Sci. Nat.* **103**, 3 (2016).
2. Yang, Z., Wang, B., Xu, C., Xu, J. & Xu, H. How Late Nights Influence Brain Cortical Structures: Distinct Neuroanatomical Measures Associated With Late Chronotype in Young Adults. *Brain Topogr.* **38**, 9 (2025).
3. Horne, J. A. & Ostberg, O. A self-assessment questionnaire to determine morningness-eveningness in human circadian rhythms. *Int. J. Chronobiol.* **4**, 97–110 (1976).
4. Yatagan Sevim, G., Law, T. Y. & Evans, S. L. Mindfulness mediates the association between chronotype and depressive symptoms in young adults. *PLOS ONE* **20**, e0319915 (2025).
5. Morris, S. M. J. & Kountouriotis, G. K. Anxiety in emerging adults: The role of chronotype, emotional competence, and sleep quality. *Chronobiol. Int.* **41**, 1566–1573 (2024).
6. Adan, A. *et al.* Circadian Typology: A Comprehensive Review. *Chronobiol. Int.* **29**, 1153–1175 (2012).
7. Caci, H., Robert, P. & Boyer, P. Novelty seekers and impulsive subjects are low in morningness. *Eur. Psychiatry* **19**, 79–84 (2004).
8. Carciofo, R. Morning affect, eveningness, and amplitude distinctness: associations with negative emotionality, including the mediating roles of sleep quality, personality, and metacognitive beliefs. *Chronobiol. Int.* **37**, 1565–1579 (2020).
9. Byrne, J. E. M. *et al.* Circadian modulation of human reward function: Is there an evidentiary signal in existing neuroimaging studies? *Neurosci. Biobehav. Rev.* **99**, 251–274 (2019).
10. Hasler, B. P., Sitnick, S. L., Shaw, D. S. & Forbes, E. E. An altered neural response to reward may contribute to alcohol problems among late adolescents with an evening chronotype. *Psychiatry Res. Neuroimaging* **214**, 357–364 (2013).
11. Forbes, E. E. *et al.* PER2 rs2304672 Polymorphism Moderates Circadian-Relevant Reward Circuitry Activity in Adolescents. *Biol. Psychiatry* **71**, 451–457 (2012).
12. Hasler, B. P., Casement, M. D., Sitnick, S. L., Shaw, D. S. & Forbes, E. E. Eveningness among late adolescent males predicts neural reactivity to reward and alcohol dependence 2 years later. *Behav. Brain Res.* **327**, 112–120 (2017).
13. Spielberg, J. M., Heller, W., Silton, R. L., Stewart, J. L. & Miller, G. A. Approach and Avoidance Profiles Distinguish Dimensions of Anxiety and Depression. *Cogn. Ther. Res.* **35**, 359–371 (2011).
14. Kanazawa, S. & Perina, K. Why night owls are more intelligent. *Personal. Individ. Differ.* **47**, 685–690 (2009).
15. Roberts, R. D. & Kyllonen, P. C. Morningness–eveningness and intelligence: early to bed, early to rise will likely make you anything but wise! *Personal. Individ. Differ.* **27**, 1123–1133 (1999).
16. Song, J. & Stough, C. The relationship between morningness–eveningness, time-of-day, speed of information processing, and intelligence. *Personal. Individ. Differ.* **29**, 1179–1190 (2000).
17. Schmidt, C. *et al.* Pushing the Limits: Chronotype and Time of Day Modulate Working Memory-Dependent Cerebral Activity. *Front. Neurol.* **6** (2015).
18. Díaz-Morales, J. F. & Escribano, C. Predicting school achievement: The role of inductive reasoning, sleep length and morningness–eveningness. *Personal. Individ. Differ.* **55**, 106–111 (2013).
19. Preckel, F., Lipnevich, A. A., Schneider, S. & Roberts, R. D. Chronotype, cognitive abilities, and academic achievement: A meta-analytic investigation. *Learn. Individ. Differ.* **21**, 483–492 (2011).
20. Randler, C., Díaz-Morales, J. F., Rahafar, A. & Vollmer, C. Morningness–eveningness and amplitude – development and validation of an improved composite scale to measure circadian preference and stability (MESSi). *Chronobiol. Int.* **33**, 832–848 (2016).
21. Oginska, H., Mojsa-Kaja, J. & Mairesse, O. Chronotype description: In search of a solid subjective amplitude scale. *Chronobiol. Int.* **34**, 1388–1400 (2017).
22. Puig-Navarro, Y., Arrona-Palacios, A. & Díaz-Morales, J. F. The relevance of morning affect, eveningness and distinctness in regard to the mental health of adolescents. *Chronobiol. Int.* **42**, 340–350 (2025).
23. Carciofo, R. & Song, N. The Chinese Morningness-Eveningness-Stability-Scale improved (MESSi): validity, reliability, and associations with sleep quality, personality, affect and life satisfaction. *Chronobiol. Int.* **36**, 1036–1046 (2019).
24. Díaz-Morales, J. F., Randler, C., Arrona-Palacios, A. & Adan, A. Validation of the MESSi among adult workers and young students: General health and personality correlates. *Chronobiol. Int.* **34**, 1288–1299 (2017).

25. Zareba, M. R. *et al.* The subjective amplitude of the diurnal rhythm matters - chronobiological insights for neuroimaging studies. *Behav. Brain Res.* 114640 https://doi.org/10.1016/j.bbr.2023.114640 (2023).
26. Oldham, S. *et al.* The anticipation and outcome phases of reward and loss processing: A neuroimaging meta-analysis of the monetary incentive delay task. *Hum. Brain Mapp.* **39**, 3398–3418 (2018).
27. Knutson, B., Westdorp, A., Kaiser, E. & Hommer, D. FMRI Visualization of Brain Activity during a Monetary Incentive Delay Task. *NeuroImage* **12**, 20–27 (2000).
28. Scislewska, P. *et al.* High distinctness of circadian rhythm is related to negative emotionality and enhanced neural processing of punishment-related information in men. *bioRxiv* 2024.09.13.612861 https://doi.org/10.1101/2024.09.13.612861 (2024).
29. Stoet, G. PsyToolkit: A software package for programming psychological experiments using Linux. *Behav. Res. Methods* **42**, 1096–1104 (2010).
30. Stoet, G. PsyToolkit: A Novel Web-Based Method for Running Online Questionnaires and Reaction-Time Experiments. *Teach. Psychol.* **44**, 24–31 (2017).
31. Gorgol, J., Waleriańczyk, W. & Randler, C. Exploring the associations between the Morningness-Eveningness-Stability-Scale improved (MESSi) and the higher-order personality factors. *Chronobiol. Int.* 1–12 https://doi.org/10.1080/07420528.2023.2212043 (2023).
32. Fornal-Pawlowska, M., Wolynczyk-Gmaj, D. & Szelenberger, W. Validation of the Polish version of the Athens Insomnia Scale. *Psychiatr Pol* **45**, 211–219 (2011).
33. Torrubia, R., Ávila, C., Moltó, J. & Caseras, X. The Sensitivity to Punishment and Sensitivity to Reward Questionnaire (SPSRQ) as a measure of Gray's anxiety and impulsivity dimensions. *Personal. Individ. Differ.* **31**, 837–862 (2001).
34. Wytykowska, A., Białaszek, W. & Ostaszewski, P. Psychometryczne właściwości polskiej wersji krótkiej skali Wrażliwości Na Kary i Nagrody (SPSRQ-SF Cooper i Gomez, 2008). https://doi.org/10.2478/v10167-010-0083-6 (2014).
35. Jr, P. T. C. & McCrae, R. R. Revised NEO personality inventory (NEO-PI-R) and NEO five-factor (NEO-FFI) inventory professional manual. *Odessa Fl PAR* (1992).
36. Zawadzki, B., Strelau, J., Szczepaniak, P. & Śliwińska, M. Inwentarz osobowości NEO-FFI Costy i McCrae. *Adapt. Pol. Podręcznik Warszawa Prac. Testów Psychol. PTP* (1998).
37. Carver, C. S. & White, T. L. Behavioral inhibition, behavioral activation, and affective responses to impending reward and punishment: The BIS/BAS Scales. *J. Pers. Soc. Psychol.* **67**, 319–333 (1994).
38. Müller, J. M. & Wytykowska, A. M. Psychometric properties and validation of a Polish adaptation of Carver and White's BIS/BAS scales. *Personal. Individ. Differ.* **39**, 795–805 (2005).
39. Crawford, J. R. & Henry, J. D. The Positive and Negative Affect Schedule (PANAS): Construct validity, measurement properties and normative data in a large non-clinical sample. *Br. J. Clin. Psychol.* **43**, 245–265 (2004).
40. Fajkowska, M. & Marszał-Wiśniewska, M. Właściwości psychometryczne Skali Pozytywnego i Negatywnego Afektu – Wersja Rozszerzona (PANAS-X). Wstępne wyniki badań w polskiej próbie*. (2009).
41. Spitzer, R. L., Kroenke, K., Williams, J. B. W. & Löwe, B. A Brief Measure for Assessing Generalized Anxiety Disorder: The GAD-7. *Arch. Intern. Med.* **166**, 1092 (2006).
42. Kessler, R. C. *et al.* The World Health Organization adult ADHD self-report scale (ASRS): a short screening scale for use in the general population. *Psychol. Med.* **35**, 245–256 (2005).
43. Szaniawska, M. & Teodorowicz, M. Adult ADHD Self-Report Scale (ASRS-v1.1) - polska wersja. (2023).
44. Li, X., Morgan, P. S., Ashburner, J., Smith, J. & Rorden, C. The first step for neuroimaging data analysis: DICOM to NIfTI conversion. *J. Neurosci. Methods* **264**, 47–56 (2016).
45. Gulban, O. F. *et al.* poldracklab/pydeface: PyDeface v2.0.2. *Zenodo* https://doi.org/10.5281/ZENODO.3524400 (2022).
46. Scislewska, P. *et al.* Monetary Incentive Delay task - structural and functional images of 37 men; study of associations between circadian characteristics (eveningness, distinctness) and affective processing. *Openneuro.* https://doi.org/10.18112/OPENNEURO.DS005479.V1.0.3 (2024).
47. Gorgolewski, K. J. *et al.* The brain imaging data structure, a format for organizing and describing outputs of neuroimaging experiments. *Sci. Data* **3**, 160044 (2016).
48. Smith, S. M. *et al.* Advances in functional and structural MR image analysis and implementation as FSL. *NeuroImage* **23**, S208–S219 (2004).
49. Power, J. D., Barnes, K. A., Snyder, A. Z., Schlaggar, B. L. & Petersen, S. E. Spurious but systematic correlations in functional connectivity MRI networks arise from subject motion. *NeuroImage* **59**, 2142–2154 (2012).
50. Phạm, D., McDonald, D. J., Ding, L., Nebel, M. B. & Mejia, A. F. Less is more: balancing noise reduction and data retention in fMRI with data-driven scrubbing. *NeuroImage* **270**, 119972 (2023).
51. Afyouni, S. & Nichols, T. E. Insight and inference for DVARS. *NeuroImage* **172**, 291–312 (2018).

Acknowledgements

Author contributions

P.S.: Conceptualization, Study design, Methodology, Funding acquisition, Participant recruitment, Data collection, Formal analysis, Writing - Original Draft, Visualization, Figures preparation, M.R.Z.: Conceptualization, Methodology, Writing - review & editing J.L.: Participant recruitment, Data collection, Writing - review & editing A.E.S.: Writing - review & editing, Supervision, P.B.: Writing - review & editing, Supervision, I.S.: Conceptualization, Study design, Writing - review & editing, Supervision.

Competing interests

The authors declare no competing interests.

Additional information

Correspondence and requests for materials should be addressed to P.S.

Reprints and permissions information is available at www.nature.com/reprints.

Publisher's note Springer Nature remains neutral with regard to jurisdictional claims in published maps and institutional affiliations.